Wind Engineering Joint Usage/Research Center
FY2021 Research Result Report

Research Field: Wind Hazard Mitigation・Wind-Resistant Construction field
Research Year: FY2021
Research Number: 21212006
Research Theme: Effects of incoming turbulent flow on across-wind response of square-section super-tall buildings and identification of aerodynamic damping

Representative Researcher: Qingshan, Yang

Budget [FY2021]: 475,000 Yen

*There is no limitation of the number of pages of this report.
*Figures can be included to the report and they can also be colored.
*Submitted reports will be uploaded to the JURC Homepage.

1. Research Aim

With the application of new lightweight and high-strength building materials, the construction height and aspect ratio of high-rise buildings are increase, and the structural stiffness, natural vibration frequency and structural damping are decrease, which feature high-rise building with the characteristics of low damping and high flexibility, and make the high-rise buildings are typical wind sensitive structure. For example, many high-rise buildings with large aspect ratio are close to or exceed the height of atmospheric boundary layer and are directly exposure to high wind speed airflow for long period (Fig. 1). The key points of wind resistance design of high-rise building structures caused by this have attracted extensive attention.

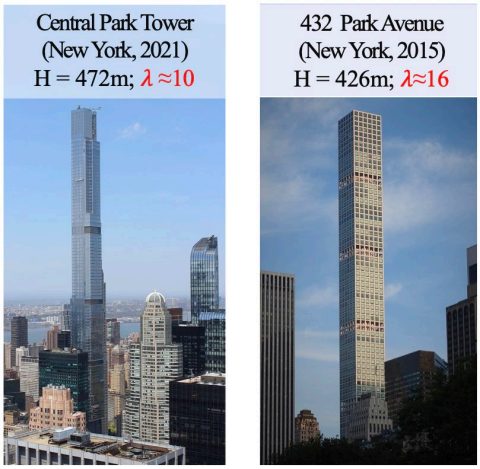

Fig. 1 High-rise buildings with super large aspect ratios

As shown in previous research, incoming turbulence is an important parameter to determine the flow characteristics around squared-section high-rise buildings. It directly affects the development of shear layer, the location of separation point and reattachment, which has a significant impact on wind load and the dynamic response of high-rise buildings. There are many previous researches have focused on the effects of turbulence on wind pressures or wind loads on 2-D isolated square prism (Lee, 1975; et. al.), 3-D isolated square prism (Kareem and Cermak, 1984; et. al.), and aerodynamic interference of 3-D square tall buildings (Bailey and Kwok, 1985; et. al.). However, there are rare researches focused on the wind-induced response affected by turbulence intensity. Moreover, we can see from Fig. 1 that

the buildings with large aspect ratios were usually constructed in the urban area, but past researches usually carried out under the open terrain or sub-urban terrain, only very less researches focused on the urban terrain.
Thus, this research aim is to investigate the effects of approaching turbulent flow on characteristics of wind-induced vibration and aerodynamic damping of the square-section super-tall buildings.

2. Research Method

2.1 Wind tunnel tests on aeroelastic models of high-rise building

The wind tunnel tests on aeroelastic high-rise building models are carried in a closed-circuit type boundary-layer wind tunnel of Beijing Jiaotong University, whose test section is 3.0 m wide, 2.0 m high, and 15 m long. With respect to the approaching turbulent boundary layer flow, the sub-urban terrain and urban terrain are considered in this study, which is simulated by spires and roughness blocks, as shown in Fig. 2. The aspect ratio λ of the two squared high-rise building models are 12 and 20. The simulated mean wind speed and turbulence intensity are shown in Fig. 3(a&b), Fig. 3(c) illustrates the power spectral density function of the simulated suburban flow at the model height, and it matches Karman spectrum very well. The mean wind speeds and turbulence intensities at the model heights located in suburban flow and urban flow are shown in Table 1.

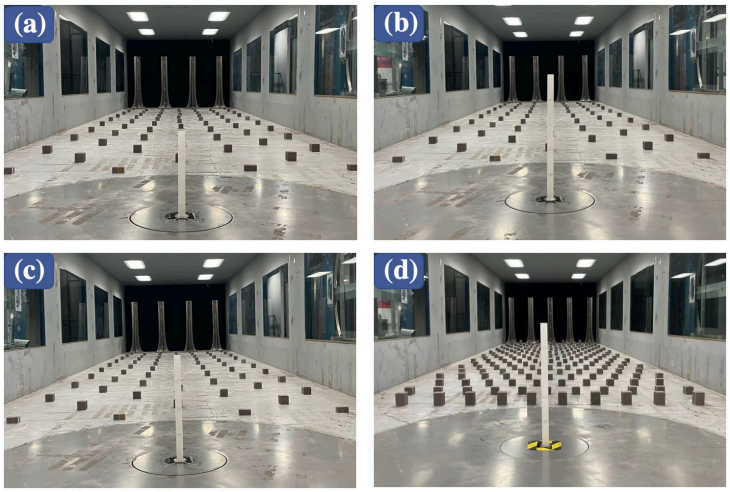

Fig. 2 Experimental model installed in the wind tunnel at sub-urban and urban terrain: (a) Suburban terrain, aspect ratio λ=12; (b) Urban terrain, aspect ratio λ=12; (c) Suburban terrain, aspect ratio λ=20; (d) Urban terrain, aspect ratio λ=20

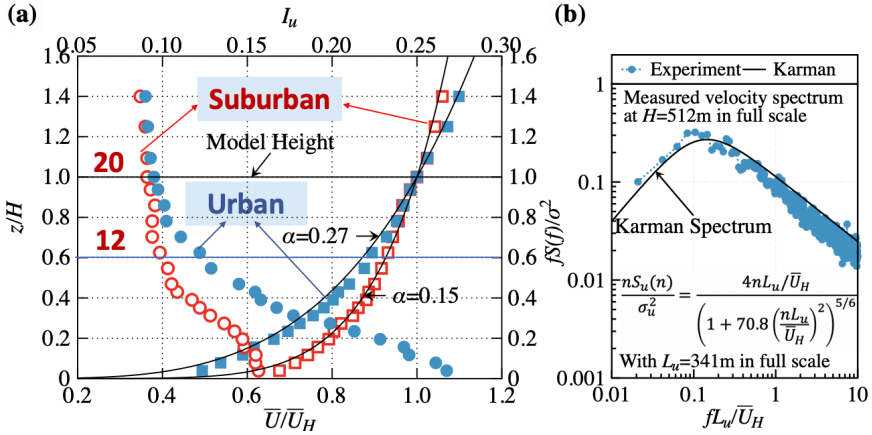

Fig. 3 Simulated sub-urban and urban flow in boundary layer wind tunnel: (a) Mean wind speed and turbulence intensity; (b) PSD for sub-urban flow

Table 1 Mean wind speed and turbulence intensity at model height

z/H	Corresponding aspect ratio λ	Sub-urban terrain		Urban terrain	
		U(m/s)	I_u(%)	U(m/s)	I_u(%)
0.6	12	9.6	9.9	8.9	12.2
1	20	10.8	9.1	10.2	9.5

The prototype size of a full-scale high-rise building are height of H=300m (aspect ratio λ=12) and 500m (aspect ratio λ=20), width of D =25m, natural frequency of around 0.15Hz, structural mass ratio of $m_{eq}/\rho B^2$=120, structural damping of 0.55% to 1.23%, and linear sway modes of vibration. The geometric scale, frequency scale and velocity scale of the wind tunnel test are set as 1/800, 80 and 1/10, respectively.

According to above requirement of dynamic similarity, the scaled models are designed, and are made of curable resin and fabricated by the 3-D print technique. By adjusting wall thickness of the test model, the mass similarity is achieved.

In order to simulate the dynamic properties such as natural frequency and structural damping, the scaled model is installed to the gimbal system shown in Fig. 4(a). As shown in Fig. 4(b), the stiffness is provided by coil springs, and structural damping is offered by the oil damper. To determine the natural frequency and structural damping of the test model, free vibration test of non-wind condition is performed and the measured free decay response is filtered within (1±0.3)f_s by a band-pass filter to eliminate influence of the noise on the free decay responses, as shown in Fig. 5. The natural frequency and structural damping of the scaled model are estimated based on the free decay response before and after the rocking model wind tunnel test. Dynamic properties of the test model are summarized in Table 2.

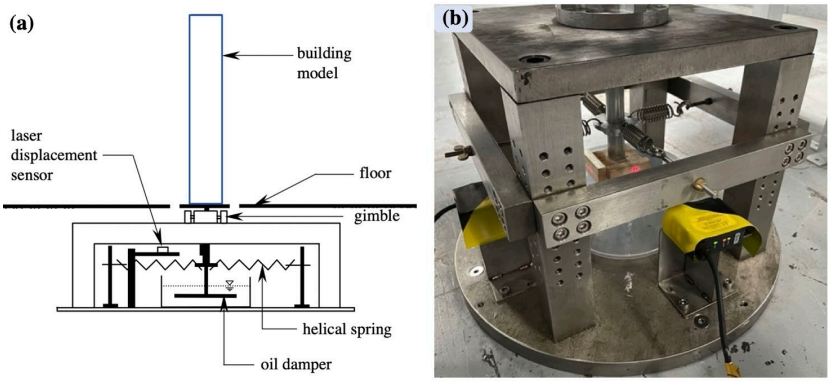

Fig. 4 Equipment of the locking aero-elastic rocking model tests: (a) Sketch of rocking model test; (b) Basement of the equipment

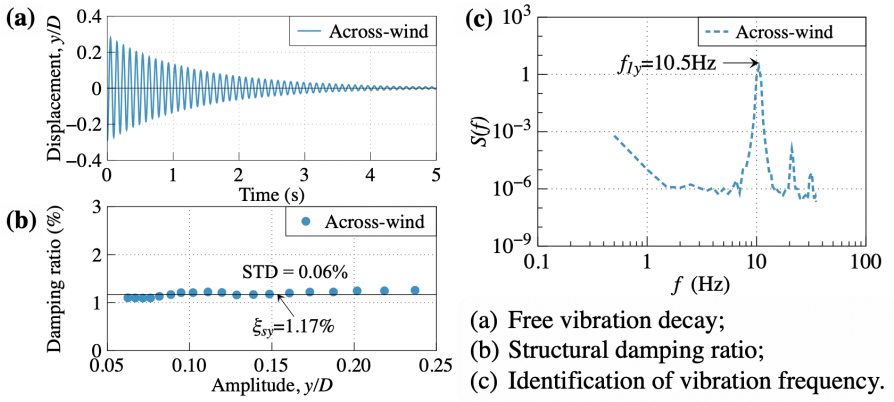

(a) Free vibration decay;
(b) Structural damping ratio;
(c) Identification of vibration frequency.

Fig. 5 Free-vibration tests on rocking model high-rise building models with aspect ratio 20

Table 2 Parameters of aeroelastic models of squared high-rise buildings

Aspect ratio	12	20
Prototype size (m^3)	25×25×300	25×25×500
Scaled size (mm^3)	32×32×384	32×32×640
Generalized mass M_s(kg)	0.0195	0.0322
Equivalent mass m_{eq}(kg/m)	0.152	0.151
Mass ratio $m_{eq}/\rho B^2$	122	121
Frequency f_s(Hz)	12.25	10.5
Structural damping ratio ξ_s(%)	0.55～1	0.55～1.23

2.2 Identification of aerodynamic damping method

Previous research show that, across-wind force acting on high-rise building include two parts: stochastic buffeting force and motion-induced force. For the stochastic buffeting force can be described in frequency domain by a spectrum. The spectrum usually can be got from High Frequency Force Balance (HFFB) and/or High Frequency Pressure Test (HFPT) in wind tunnel. Standard deviation can be obtained, too.

For the motion-induced force, one component is in phase with displacement, can further be superposed on the structural stiffness, defined as aerodynamic stiffness. However, compared with structural stiffness, the aerodynamic stiffness is much smaller, and it usually can be ignored. The other component is in phase with velocity, can further be superposed on the structural damping, and defined as aerodynamic damping. The magnitude of aerodynamic damping is comparable with structural damping. It should be noted that, aerodynamic damping becomes negative around the vortex-resonance critical speed, which acts as a source of energy input to the structure. So, it plays an important role in estimating across-wind responses of tall and slender buildings and structures.

With the assumption of that the influence of aerodynamic stiffness on across-wind response of the high-rise building can be ignored, the motion equation of the across-wind response of high-rise building can be expressed as (Chen, 2013):

$$y'' + 2(\xi_s + \xi_a)y' + y = \frac{1}{8\pi^2}\left(\frac{\rho B^2}{m_{eq}}\right)\left(\frac{1}{S_t}\right)^2\left(\frac{U}{U_{cr}}\right)^2 \eta_b \eta C_{Mb} \tag{1}$$

$$m_{eq} = \frac{M_s}{\int_0^H \phi^2(z)dz} = \frac{\int_0^H m(z)\phi^2(z)dz}{\int_0^H \phi^2(z)dz} \quad ; \qquad \eta = \frac{H}{\int_0^H \phi^2(z)dz} \tag{2}$$

where $U_{cr} = f_s B/S_t$ is the critical vortex-resonance wind speed; S_t is strouhal number and it around 0.1 for squared prism.

In Eq. (1), nonlinear aerodynamic damping is a function of both wind speed and amplitude. In this study, the generalized Van Der Pol-type (GDVP) aerodynamic damping model established by Guo et al. (2021) is adopted, and its specific expression is as follows

$$\xi_a(U, y_1) = -K_a(U, y)/(m_{eq}/\rho B^2) = \frac{\rho B^2}{m_{eq}} K_{a0}(U)\left[1 - \varepsilon(U)\cdot\left|\frac{y_1(t)}{B}\right|^{\beta(U)}\right] \tag{3}$$

Where, $K_{a0}(U)$, $\varepsilon(U)$, $\beta(U)$ are parameters used to describe the aeroelastic effect caused by structural motion. In Eq. (2), the aerodynamic damping is time-variant, which is inconveniencing to be used. Thus, the time-variant aerodynamic damping are equivalented to Eq. (3) by harmonic balance technique, where the equivalent aerodynamic damping is the function of the STD response:

$$\xi_{a,eq} = \frac{\rho B^2}{m_{eq}} K_{a0}(U)\left[1 - \varepsilon(U)\frac{\Gamma\left(\frac{\beta(U)+1}{2}\right)}{\Gamma\left(2+\frac{\beta(U)}{2}\right)\Gamma\left(\frac{1}{2}\right)}(\sqrt{2}\sigma_y/B)^{\beta(U)}\right] \tag{4}$$

In order to derive the aerodynamic damping parameters, analytical solution concerning PDF of the displacement response amplitude $f(A)$ have been deduced by employing the Equivalent Non-linear Equation (ENLE) method to solve Eq. (1), analytical solution of $f(A)$ can then be

derived as (Guo et al, 2022):

$$p(A) = CA\exp\left\{-\frac{\omega_s^3 A^2}{\pi S}\left[\xi_s - \left(\frac{\rho B^2}{m_{eq}}\right)K_{a0}\left(1 - \frac{4\varepsilon A^\beta}{(\beta+2)}\frac{\Gamma\left(\frac{3}{2}\right)\Gamma\left(\frac{\beta+1}{2}\right)}{\Gamma\left(\frac{\beta}{2}+2\right)}\right)\right]\right\} \quad (5)$$

where C is normalization constant; $A = \sqrt{\dot{y}^2/\omega_s^2 + y^2}$ is a response amplitude process; $S = \frac{1}{16\pi}\left(\frac{\rho B^2}{m_{eq}}\right)^2\left(\frac{1}{S_t}\right)^4\left(\frac{U}{U_{cr}}\right)^4 f_s^4\eta^2 S_{C_{ML}}(f_s)$ is double-sided PSD in terms of circular frequency; $S_{C_{ML}}$ is the power spectral density (PSD) function of the base bending moment coefficient; and $\Gamma(\cdot)$ is the Gamma function. Equation (5) establishes the corresponding relationship between the crosswind response of the structure and the aerodynamic damping parameters. The relationship between the probability density function of displacement response $p(y)$ and the probability density function of response amplitude $p(A)$ is as follows:

$$p(y) = \frac{1}{\pi}\int_{|y|}^{\infty}\frac{p(A)}{\sqrt{A^2 - y^2}}dA \quad (6)$$

Therefore, the aerodynamic damping parameters can be obtained by fitting the probability density function of the crosswind displacement response of the structure obtained from the wind tunnel test with Eq. (5) and (6). The equivalent aerodynamic damping can be obtained by substituting the aerodynamic damping parameters into Eq. (4); The specific expression of the probability density function of the amplitude of the displacement response in the crosswind direction of the structure can be obtained by substituting into Eq. (5).

The STD and fourth-order moment of displacement response can be calculated by the probability density function of displacement response amplitude (Chen, 2013):

$$\sigma_y = \sqrt{\frac{1}{2}E[A^2]} = \sqrt{\frac{1}{2}\int_0^A A^2 p(A)dA} \quad (7)$$

$$\alpha_{4y} = \frac{3}{8}E[A^4]/\sigma_y^4 = \frac{3}{8\sigma_y^4}\int_0^A A^4 p(A)dA \quad (8)$$

3. Research Result

3.1 Crosswind response of the high-rise building model with aspect ratio λ=20 under sub-urban terrain

From the aeroelastic experiments on high-rise building model as introduced in section 2.1, the tested results are shown as follow. It can be seen from section 2.1 that the time scale of aeroelastic test is 1/80, so the sampling time corresponding to the actual 10 minutes for one sample is 7.5s. In this study, in order to maintain the stability of data samples, the sampling time is 120s (16 samples). In order to eliminate the influence of high-frequency components, the displacement response time history is processed by low-pass filtering at 200Hz.

Fig 6 shows time history and PDF of the crosswind response of the high-rise building model with aspect ratio 20 and structural damping 1.17% in the suburban flow. From the figure, When the wind speed $\bar{U}_H/f_sB$= 8.25, less than the critical resonance wind speed $\bar{U}_{st}/f_sB$ = 10.25, the crosswind displacement response amplitude of the structure is small and shows random buffeting characteristics, the corresponding PDF shows Gaussian distribution. When the wind speed $\bar{U}_H/f_sB$= 10.21 or 12.15, closing to the critical resonance wind speed, the displacement response amplitude of the structure increases compared with that before, and the time history has the characteristics both of randomness and harmonic, showing the characteristics of mixed buffeting-harmonic vibration, the corresponding PDF can evident such kind of characteristics too. When the wind speed $\bar{U}_H/f_sB$= 14.11, larger than the critical resonance wind speed, the crosswind displacement response shows the characteristic of mixed buffeting-harmonic vibration, but contains more buffeting component than harmonic component, as evidenced by both time history and PDF.

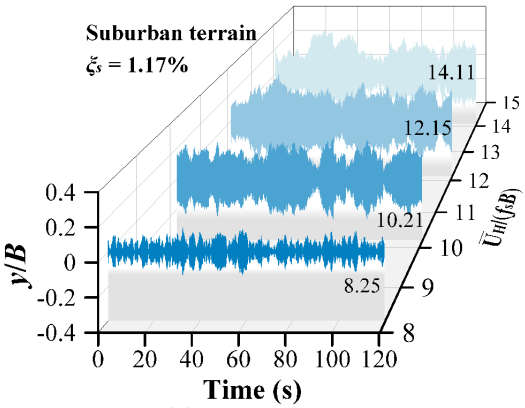

(a) Time history

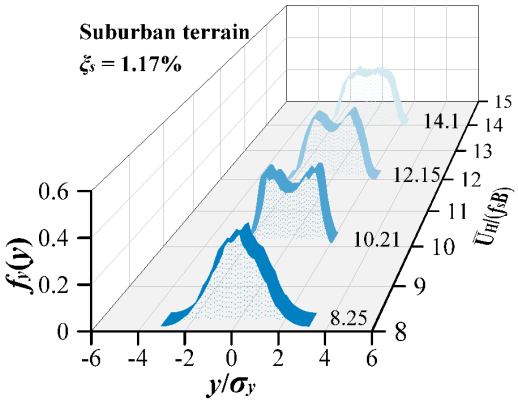

(b) Probability density function

Fig. 6 Time history and PDF of crosswind displacement samples of high-rise building with aspect ratio 20 in suburban terrain (ξ_s=1.17%)

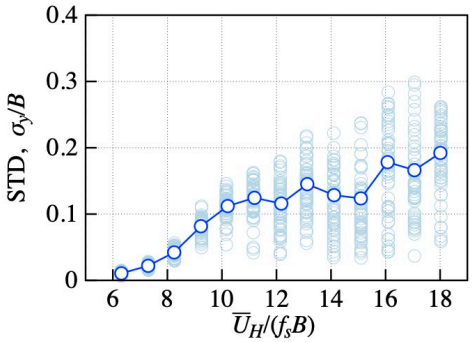

(a) STD

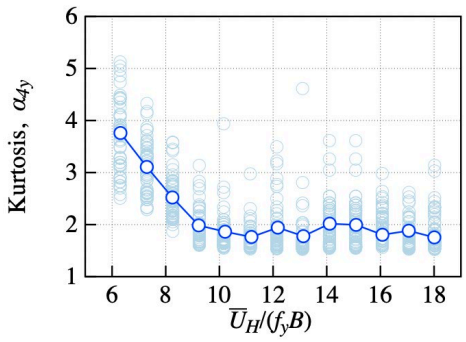

(b) Kurtosis

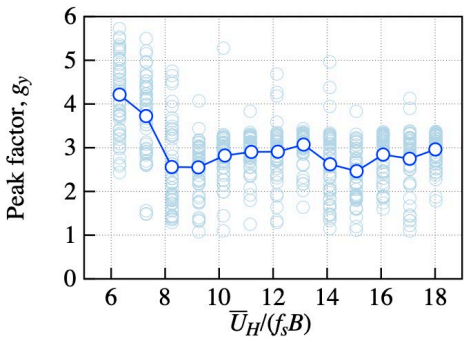

(c) Peak factor

Fig. 7 Statistic characteristics of across-wind displacement response of high-rise building with aspect ratio 20 in suburban terrain (ξ_s=1.17%)

Since the crosswind displacement response of high-rise building model is sensitive when the structural damping ξ_s=1.17%, 30 samples are collected for each wind speed. The STD response, kurtosis and peak factor, and the corresponding ensemble-averaged value for various reduced wind speeds are depicted in Fig. 7. To discuss the response characteristics at a mean level, ensemble-averaged mean values of the corresponding response statistics at various structural damping and reduced wind speed are calculated and summarized in Fig. 8. It can be seen from Fig. 8 that statistics of the crosswind response are significantly affected by the reduced wind speed $U_r = \bar{U}_H/f_sB$ and structural damping ξ_s. Fig. 8(a) displays the ensemble-averaged RMS response σ_y with various structural damping and it can be observed that σ_y decreases with increase of structural damping ξ_s. Moreover, it can be seen from Fig. 8(b) and (c) that tendency of the response kurtosis is similar to that of the peak factor. When the wind speed is away from the vortex resonance critical wind speed (U_{st}=10.25),

the kurtosis is around 3 and the peak factor is 3.5~4, indicating that the crosswind response is random Gaussian and the stochastic buffeting force dominates the response. Both the kurtosis and peak factor decrease significantly when the wind speed is around U_{st}=10.25, indicating that the aerodynamic damping begins to play a dominant role in the crosswind response. With a further increase of wind speed, both the kurtosis and peak factor are significantly affected by the structural damping ξ_s.

For instance of reduced wind speed U_r=18, the kurtosis and peak factor are 1.6 and 1.8 for ξ_s=0.56%, while are 2.3 and 3.0 forξ_s=1.23%, reflecting that aerodynamic damping dominates the response when the structural damping is low while the stochastic buffeting force is dominant for large structural damping at a relatively high reduced wind speeds.

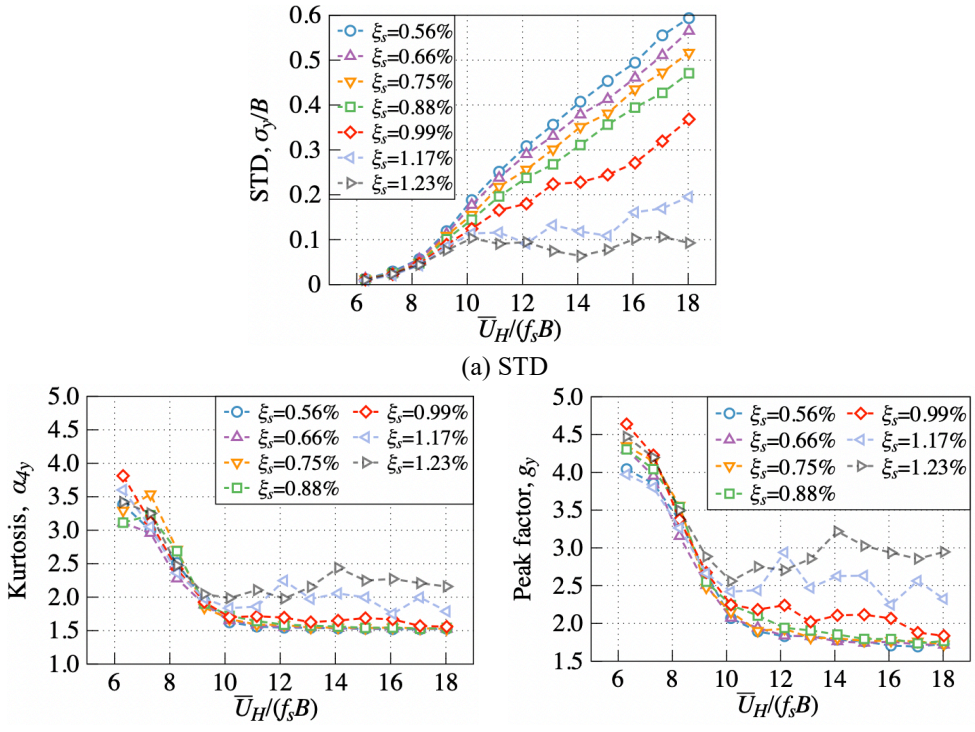

(a) STD

(b) Kurtosis (c) Peak factor

Fig. 8 Statistic characteristics of across-wind displacement response of high-rise building with aspect ratio 20 in suburban terrain (ξ_s=0.56%, 0.66%, 0.75%, 0.88%, 0.99%, 1.17%, 1.23%)

3.2 Effects of incoming turbulence on crosswind response of the high-rise building model

In section 3.1, the statistic characteristics of crosswind displacement response of squared high-rise building are introduced. This section illustrates the effects of the incoming turbulence for the building model with aspect ratio 12 and 20, respectively.

3.2.1 Aspect ratio 12

Fig. 9 shows the effects of incoming flow on across-wind displacement response of high-rise building with aspect ratio 12 under suburban and urban flow. RMS response, skewness, and peak factor of are compared when the structural damping ξ_s=0.54%, 0.67%, 1.01%.

It can be seen in the figure that, when the structural damping ratio is small (ξ_s=0.54%), and the wind speed is less than the critical resonance wind speed, the crosswind displacement response of the structure under both suburban and urban flows shows random buffeting characteristics, and the kurtosis and peak factor are close to 3 and 3.5 respectively, which also corresponds to the Gaussian response; When the wind speed exceeds and is far away from the critical resonance wind speed, the response under suburban terrain shows harmonic characteristics, and the kurtosis and peak factor are close to 1.5, while the response under urban flow mainly shows buffeting characteristics, and the kurtosis and peak factor are 2.5

and 3, respectively. In addition, the RMS response under suburban terrain is significantly greater than that from urban terrain. It can be seen that under low damping and high wind speed, the increase of turbulence suppresses the crosswind aeroelastic effect of square high-rise buildings with aspect ratio of 12. This conclusion is also the same as that under similar test conditions in previous studies.

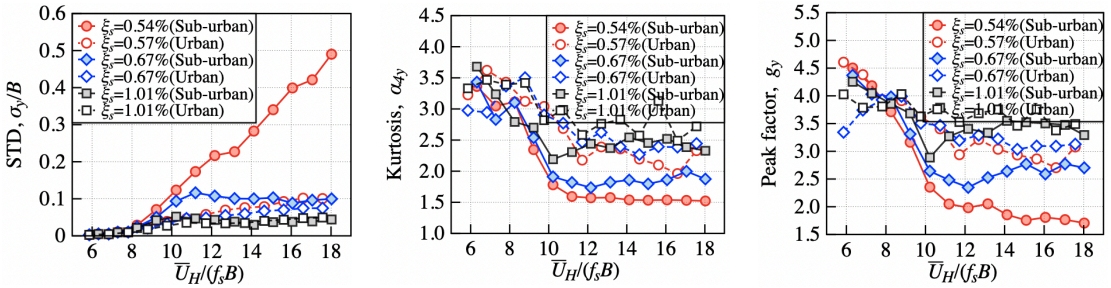

(a) STD (b) Skewness (c) Peak factor

Fig. 10 Effects of incoming flow on across-wind displacement response of high-rise building with aspect ratio 12 under suburban and urban flow

According to the above, the crosswind response of high-rise building with aspect ratio 12 is significantly influenced by the incoming turbulence. In order to analyze the causes of the above differences and clarify the specific impact of the increase of turbulence on the crosswind displacement response, Fig. 10 shows the PSD of crosswind displacement in suburban and urban terrain of high-rise building with aspect ratio 12 when the structural damping ratio ξ_S=0.54%.

For the low incoming turbulence case as shown in the Fig. 10(a), when the wind speed is less than the critical resonance wind speed, there are two spectral peaks corresponding to vortex shedding frequency (left) and structural natural vibration frequency (right), and the structural response is random buffeting. As the wind speed near the critical resonance wind speed, the vortex shedding frequency is "locked" by the structural vibration frequency within a certain wind speed range, so that there is only one spectral peak in the displacement response PSD, and the structural response is harmonic vibration. When the wind speed continues to increase to far away from the critical wind speed of vortex induced resonance, there is still only one spectral peak corresponding to the natural vibration frequency of the structure in the displacement response power spectrum, and the vortex shedding frequency cannot be separated from it, the response shows harmonic vibration.

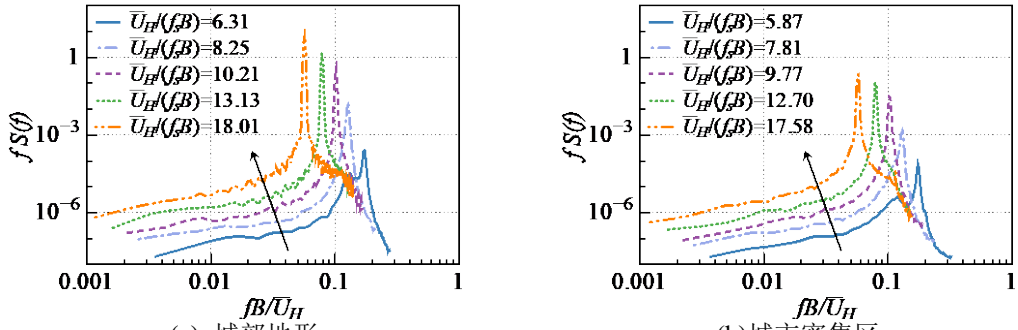

(a) 城郊地形 (b)城市密集区

Fig. 11 PSD of across-wind displacement in suburban and urban terrain of high-rise building with aspect ratio 12

For the high incoming turbulence case as shown in the Fig. 10(b), The result of the small wind speed shows the same regular with that of low incoming turbulence. When the wind speed is near the critical wind speed of vortex shedding, there is only one spectral peak in the displacement response power spectrum. Combined with the response time history and probability density function under this condition, it can be seen that there are few harmonic components in the response at this time, mainly showing buffeting characteristics. When the wind speed continues to increase, there are two spectral peaks corresponding to the

structural vibration frequency (left) and vortex shedding frequency (right) in the displacement response power spectrum, indicating that the vortex shedding frequency is separated from the structural vibration frequency, and the response shows the characteristics of random buffeting.

From the above analysis, it can be seen that for squared-section high-rise buildings with aspect ratio of 12, the increase of turbulence suppresses the vortex shedding intensity on the sideward surface, thus suppresses the occurrence of vortex induced resonance.

3.2.2 Aspect ratio 20

As described in section 3.2.1, the vibration characteristics of high-rise buildings with aspect ratio of 12 are quite different under the two terrain. Fig.11 shows the effects of incoming flow on across-wind displacement response of high-rise building with aspect ratio 20 under suburban and urban flow when the structural damping ratio is similar (ξ_S=0.56%, 0.99%, 1.23%). The figure shows that the vibration form of crosswind response of squared-section high-rise buildings with aspect ratio of 20 in suburban and urban terrain has not been changed, but only the vibration amplitude decreases. The reason of the crosswind response of high-rise buildings with super large aspect ratio isn't affected much by turbulence can be determined by the position of the structure in the wind field (Fig. 3). The turbulence intensity of two terrains at the top 20% height of high-rise buildings with aspect ratio 20 are almost the same, thus their influence to crosswind response aren't significantly. As a conclusion, in the wind resistant design of high-rise buildings with large aspect ratio, we should also pay attention to the crosswind response under high turbulence.

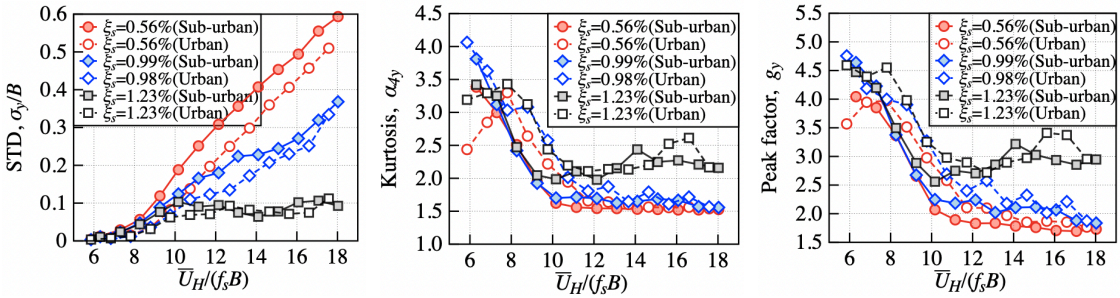

(a) STD (b) Skewness (c) Peak factor

Fig. 12 Effects of incoming flow on across-wind displacement response of high-rise building with aspect ratio 20 under suburban and urban flow

3.3 Effects of incoming turbulence on aerodynamic damping of the high-rise building model

3.3.1 Validation of the aerodynamic damping identification method

To validate the accuracy of identified aerodynamic damping by the method introduced in the section 2.2, the identified aerodynamic damping from free-vibration tests were compared to the results from that of forced-vibration test.

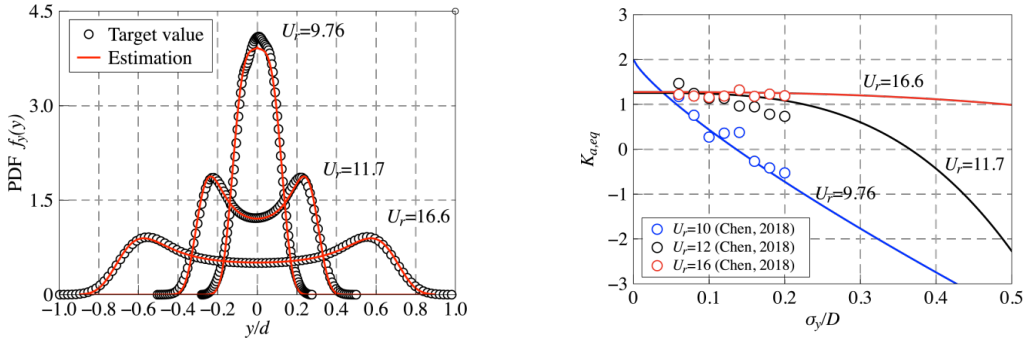

(a) PDF (b) $K_{a,eq}$

Fig. 13 Validation of the aerodynamic damping identification

As shown in Fig. 13(a), the PDF of crosswind displacement response of high-rise building with aspect ratio 20 when the structural damping ratio is 0.56%, when the reduced wind speed U_r=9.76、11.7、16.6. The PDF are estimated with the form of Eq. (5) by least-square technique. Thus, the aerodynamic damping parameters can be derived and $K_{a,eq}$ can be derived and shown in Fig. 13(b). Compared to a similar case from Chen et al. (2018) which performed by the forced vibration test, the results show good agreement when the wind speed U_r=9.76、16.6. However, the vibration isn't stable when wind speed U_r=11.7, so the equivalent aerodynamic damping ratio has some difference from that of the forced vibration test. The above aerodynamic damping at each wind speed is estimated by a fixed structural damping ratio. The identified aerodynamic damping also can be used to estimate the crosswind response at other structural damping level, as shown in Fig. 14. The results show that, the STD response can be estimated well at each wind speed and structural damping less than 1%, but the skewness and peak factor can only be estimated well when the harmonic vibration is dominant.

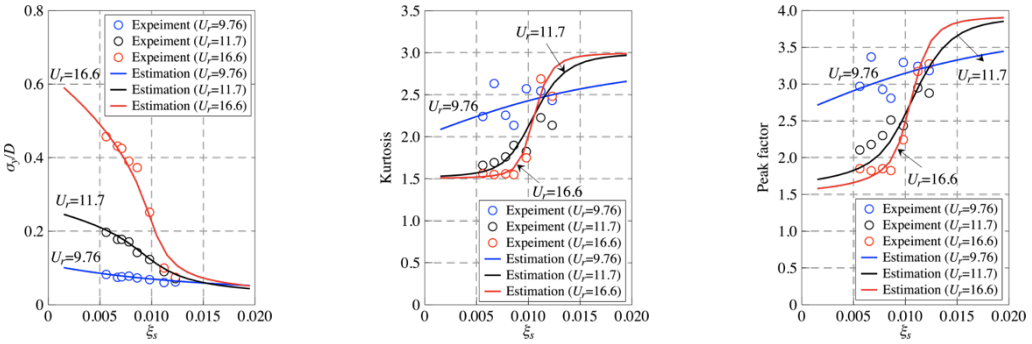

(a) STD (b) Kurtosis (c) Peak factor

Fig. 14 Identification of aerodynamic damping of 12 high-rise building under suburban flow (U_r=9.76、11.7、16.6)

3.3.2 Aspect ratio 12

As shown in the section 3.2.1, the aeroelastic effects of the squared-section high-rise building with aspect ratio 12 is suppressed when the incoming turbulence is large. Thus, the aerodynamic damping only exists when high-rise building with aspect ratio 12 located in the suburban terrain.

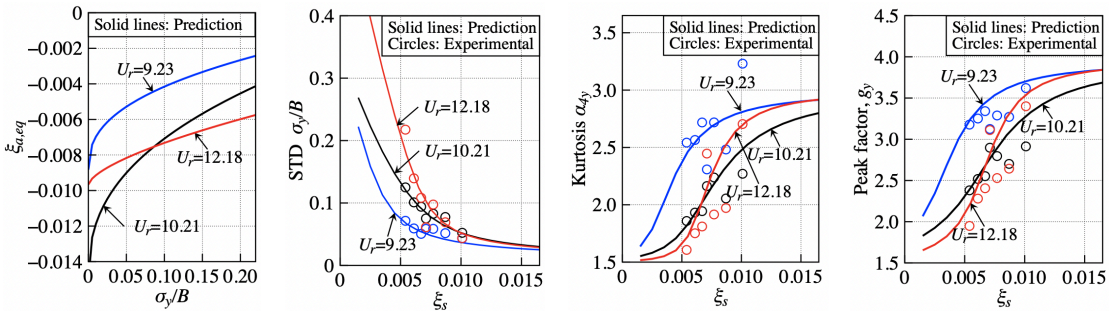

a1) $\xi_{a,eq}$ a2) STD a3) Kurtosis a4) Peak factor

(a) U_r =9.23、10.21、12.18

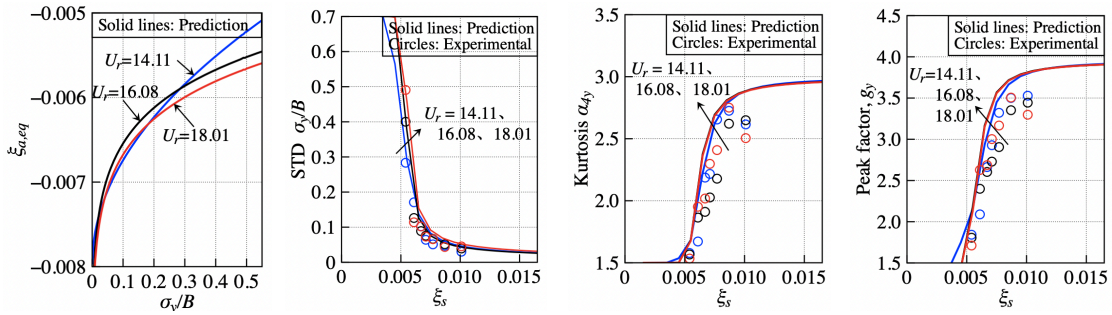

b1) $\xi_{a,eq}$ b2) STD b3) Kurtosis b4) Peak factor

(b) U_r=14.11、16.08、18.01

Fig. 15 Identification of aerodynamic damping of 12 high-rise building in suburban flow

The identified equivalent aerodynamic damping shows nonlinear characteristics for each wind speed. The predicted STD response, skewness and peak factor agree with the experimental results when the harmonic component is dominant.

3.3.3 Aspect ratio 20

Fig. 16 shows the effects of the incoming turbulence on equivalent aerodynamic damping of squared-section tall buildings with aspect ratio 20 under suburban and urban flow. It can be known that, when the wind speed is less than the critical resonance wind speed under two incoming flows, the variation trend of crosswind aerodynamic damping of high-rise buildings with aspect ratio of 20 in urban terrain is significantly different from that in suburban terrain. The increase of turbulence makes the aerodynamic damping significantly reduced. When the wind speed U_r=11.19~12.18(SU), the crosswind aerodynamic damping under two incoming flows convert to be with a positive curvature. The crosswind aerodynamic damping has small difference when the wind speed is larger, corresponding to the same amplitude under the two incoming flows. When converting wind speed U_r =17.06~18.01 (SU), the crosswind aerodynamic damping corresponding to the same amplitude in both suburban and urban terrain are roughly the same. The above shows that when the wind speed is relatively small, the increase of turbulence reduces the cross wind aerodynamic damping of high-rise buildings with aspect ratio of 20 to a certain extent, while when the wind speed increases, the turbulence almost no longer affects the crosswind aerodynamic damping of high-rise buildings with slenderness ratio of 20.

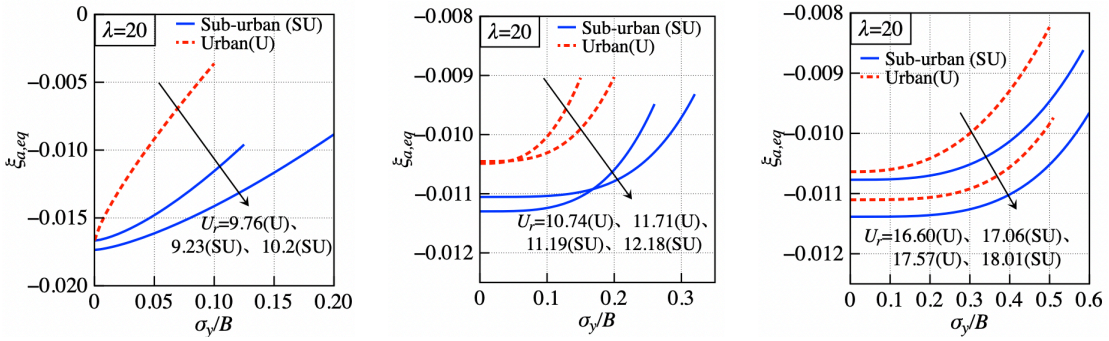

(a) U_r =9.23~10.2(SU) (b) U_r =11.19~12.18(SU) (c) U_r =17.06~18.01(SU)

Fig. 17 Aerodynamic damping of tall buildings with aspect ratio 20 under suburban and urban flow

4. Published Paper etc.

[Underline the representative researcher and collaborate researchers]
[Published papers]
1.
2.

[Presentations at academic societies]
1.
2.

[Published books]
1.
2.

[Other]
Intellectual property rights, Homepage etc.

5. Research Group

1. Representative Researcher
   Qingshan, Yang
2. Collaborate Researchers
   1. Yong Chul, Kim
   2. Yukio, Tamura
   3. Wenshan, Shan
   4. Kunpeng, Guo

6. Abstract (half page)

Research Theme: Effects of incoming turbulent flow on across-wind response of square-section super-tall buildings and identification of aerodynamic damping

Representative Researcher (Affiliation): Qingshan, Yang (Chongqing University)

Summary・Figures

By wind tunnel tests on aeroelastic model of squared-section high-rise buildings with aspect rati 12 and 20, the effects of the incoming turbulence flow on the across-wind response and aerodynamic damping are investigated. The results show that:

1) For the high-rise building with aspect ratio 12, larger incoming turbulence can be suppressed the crosswind aeroelastic effects so that to eliminate the response significantly;

2) For the high-rise building with aspect ratio 20, aeroelastic effects exist under both suburban and urban terrain. When the wind speed is large, both the displacement response and aerodynamic damping are influenced limitedly.